Formation and magic number characteristics of clusters formed during solidification processes

2007 J. Phys.: Condens. Matter 19 196103

(http://iopscience.iop.org/0953-8984/19/19/196103)

IOP PUBLISHING JOURNAL OF PHYSICS: CONDENSED MATTER

J. Phys.: Condens. Matter **19** (2007) 196103 (17pp) doi:10.1088/0953-8984/19/19/196103

Formation and magic number characteristics of clusters formed during solidification processes

Rang-su Liu[1], Ke-jun Dong[1,2], Ze-an Tian[1], Hai-rong Liu[3], Ping Peng[3] and Ai-bing Yu[2]

[1] Department of Physics, Hunan University, Changsha 410082, People's Republic of China
[2] Centre for Simulation and Modelling of Particulate Systems and School of Materials Science and Engineering, The University of New South Wales, Sydney, NSW, 2052, Australia
[3] College of Materials Science and Engineering, Hunan University, Changsha 410082, People's Republic of China

Received 9 January 2007, in final form 16 March 2007
Published 17 April 2007
Online at stacks.iop.org/JPhysCM/19/196103

Abstract

A molecular dynamics simulation study has been performed for a large-sized system consisting of 10^6 liquid metal Al atoms to investigate the formation and magic number characteristics of various clusters formed during solidification processes. The cluster-type index method (CTIM) is adopted to describe various types of cluster by basic clusters. It is demonstrated that the icosahedral cluster (12 0 12 0) is the most important basic cluster, and that it plays a critical role in the microstructure transition. A new statistical method has been proposed to classify the clusters as some group levels according to the numbers of basic clusters contained in each cluster. The magic numbers can be determined by the respective peak value positions of different group levels of clusters, and the magic number sequence in the system is 13, 19, 25(27), 31(33), 38(40), 42(45), 48(51), 55(59), 61(65), 67, ... the numbers in the brackets are the second magic number of the corresponding group levels of clusters. This magic number sequence is in good agreement with the experimental results obtained by Schriver and Harris *et al*, and the experimental results can be reasonably well explained.

(Some figures in this article are in colour only in the electronic version)

1. Introduction

It is well known that one of the most striking features of cluster configurations, that has attracted much attention, is the existence of prominent peaks in their mass spectra. The clusters corresponding to prominent peaks are often considered to be rather stable because they have magic number characteristics [1]. Extensive experimental and theoretical studies have been carried out on the formation mechanisms and magic number characteristics of cluster configurations [1–16]. The experimental studies are carried out by physical or chemical methods to construct particles or clusters with dozens to hundreds of atoms in

special configurations [1–10]. The theoretical works are mainly carried out on various cluster configurations formed by accumulating atoms according to different patterns [11–16]. However, another kind of similar cluster configuration which has been found in some liquid metals during their rapid solidification processes [17–21] is also important for understanding in depth the solidification processes from liquid state to solid state. As we know, whether in experimental or theoretical studies, the formation mechanisms and magic number characteristics of cluster configurations, especially of larger cluster configurations, formed during solidification processes in liquid metals are still not well understood up to now.

The main purpose of this paper is to reveal the formation mechanisms and magic number characteristics of cluster configurations, especially of larger cluster configurations, formed during solidification processes in liquid metals. With this aim, based on our previous works [17–21], a tracking simulation study on the rapid solidification processes of a system consisting of 10^6 liquid metal Al atoms has been performed by using a molecular dynamics method, centre-atom method [17] and cluster-type index method [19, 20], and some new results have been obtained.

2. Simulation method

The molecular dynamics (MD) technique used here is based on canonical MD, and the simulation conditions are as follows: 10^6 Al atoms are placed in a cubic box and the system runs under periodic boundary conditions. The cubic box size is determined by both the number of atoms in the system and the mean volume of each atom at each given temperature, for this simulation the mean volume is taken from the Ω–T curve as shown in figure 5 of [22]; thus the box size would change with temperature. The interacting interatomic potential adopted here is the effective pair potential function of the generalized energy-independent nonlocal model-pseudopotential theory developed by Wang *et al* [23, 24]. The effective pair potential function is

$$V(r) = (Z_{\mathrm{eff}}^2/r)\left[1 - \left(\frac{2}{\pi}\right)\int_0^\infty \mathrm{d}q\, F(q)\sin(rq)/q\right] \tag{1}$$

where Z_{eff} and $F(q)$ are, respectively, the effective ionic valence and the normalized energy wavenumber characteristics [23, 24]. This pair potential is cut off at 20 au (atom unit). The time step of simulation is chosen as 10^{-15} s.

The simulation starts at 943 K (the melting point (T_{m}) of Al is 933 K). First of all, we let the system run at that temperature so as to reach an equilibrium liquid state determined by the energy change of system. Thereafter, the damped force method [25, 26] is employed to decrease the temperature of the system with the cooling rate of 1.00×10^{13} K s^{-1} to some given temperatures: 883, 833, 780, 730, 675, 625, 550, 500, 450, 400 and 350 K. At each given temperature, the instantaneous spatial coordinates of each atom are recorded for analysis below. The bond-type index method of Honeycutt–Andersen (HA) [27], the centre-atom method [17] and the cluster-type index method [19, 20] are used to detect and analyse the bond types and cluster types of the related atoms in the system, and we go further to investigate the formation mechanisms and magic number characteristics of various clusters configurations formed during solidification processes.

3. Results and discussion

3.1. Pair distribution function analyses

Since the pair distribution function $g(r)$ of atoms is a Fourier transformation of the structure factor $S(q)$ obtained from x-ray diffraction in a system, $g(r)$ can be used to compare the

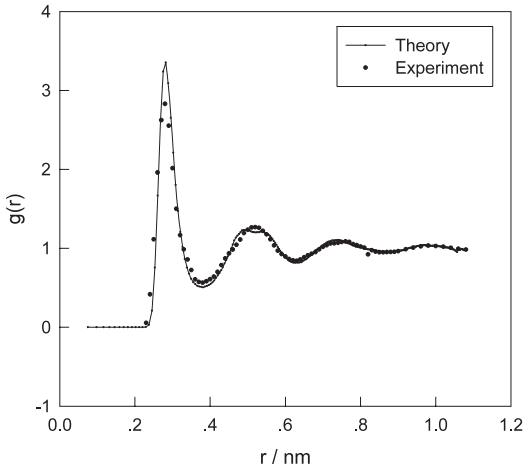

Figure 1. Pair distribution function of liquid Al at 943 K.

Table 1. Relations of the number of various bond types (%) with temperature (K).

Temp (K)	Bond types and corresponding relative numbers (%)													
	1201	1211	1301	1311	1321	1331	1421	1422	1431	1441	1541	1551	1661	1771
943	1.6	1.5	1.0	7.2	7.2	0.7	3.3	7.1	21.2	4.4	13.2	14.3	4.5	0.1
883	1.5	1.4	0.9	6.9	7.0	0.6	3.2	6.9	21.3	4.5	13.5	15.2	4.7	0.1
833	1.3	1.3	0.9	6.5	6.7	0.6	3.1	6.8	21.3	4.5	13.7	16.3	4.9	0.1
780	1.2	1.2	0.8	6.1	6.4	0.5	3.0	6.5	21.3	4.6	13.9	17.7	5.1	0.1
730	1.1	1.1	0.7	5.7	6.1	0.5	2.9	6.3	21.2	4.6	14.1	19.1	5.4	0.1
675	0.9	0.9	0.7	5.2	5.7	0.5	2.8	6.0	21.1	4.6	14.3	20.9	5.6	0.1
625	0.9	0.9	0.6	5.1	5.6	0.4	2.7	5.9	21.1	4.5	14.5	22.0	5.7	0.1
550	0.9	0.9	0.6	4.8	5.4	0.4	2.6	5.7	21.0	4.3	14.6	24.0	5.7	0.1
500	0.8	0.9	0.6	4.7	5.4	0.3	2.5	5.6	21.1	4.1	14.6	25.3	5.6	0.1
450	0.8	0.9	0.5	4.5	5.3	0.3	2.4	5.4	21.0	3.9	14.6	26.8	5.6	0.0
400	0.7	0.9	0.5	4.3	5.2	0.3	2.3	5.3	20.9	3.8	14.6	28.2	5.6	0.0
350	0.7	0.9	0.5	4.2	5.2	0.3	2.2	5.1	20.8	3.6	14.6	29.4	5.5	0.0

theoretical results with the experimental ones for liquid and amorphous structures. Figure 1 shows the pair distribution function $g(r)$ of the simulating system at 943 K and the experimental result obtained by Waseda [28]. It can be clearly seen that the simulation result is in good agreement with the experimental result. This means that the effective pair-potential function adopted here is rather successful for describing the physical nature of the system.

3.2. Bond-type index analyses

At present, the pair analysis technique is an important method for describing and discerning the concrete relationship of an atom with its near neighbours in liquid and amorphous systems, and the Honeycutt–Andersen (HA) bond-type indices [27] have been successfully applied to describe and analyse microstructure transitions in simulation systems [18, 19]. In this simulation for a system consisting of 10^6 Al atoms, various bond types are also described by HA indices, as shown in table 1.

From table 1, some results can be observed and compared with those described previously in [19] for a system consisting of 4×10^5 Al atoms as follows.

Firstly, the relative numbers of 1551 and 1541 bond types, related to the icosahedral configurations and amorphous structures, represent 14.3% and 13.2% at 943 K, respectively, and the two bond types represent 27.5% of the total bond types. It is worth noting that these percentages change with the system temperature. At 350 K, the proportion of 1551 bond type increases remarkably with decreasing temperature, reaching 29.4% of the total, whilst the 1541 bond type only increases slightly to 14.6% of the total; the sum of the 1551 and 1541 bond types makes up 44.0% of all bond types, indicating an increase of 16.5% from the corresponding proportion at 943 K. The 1551 bond type, however, still plays a decisive role in the evolution process of microstructures, as shown previously in table 1 of [19].

For the relative numbers of the 1441, 1431, 1421 and 1422 bond types related to the tetrahedral structures, the 1331, 1321, 1311 and 1301 bond types related to the rhombohedral structures, and the 1661 bond type related to hcp and bcc structures, are also similar to those obtained from previous works as mentioned above.

Highly interesting is the 1771 bond type; according to the definition of Honeycutt–Andersen bond-type indices, it should possess seven-fold symmetry. It is well known that seven-fold symmetry cannot exist in the crystal solid state. Although the relative number of 1771 bond types is less than 0.1%, it still only exists in liquid and supercooled liquid states above 500 K, and disappears in the solid state below 500 K. This result just proves that seven-fold symmetry cannot exist in the crystal solid state, and further proves that seven-fold symmetry also cannot exist in amorphous solid state.

On the whole, these simulation results are rather close to those obtained in our previous works on different-sized liquid metal systems [17–21]; that is to say, for different-sized liquid metal systems, the simulation results of relative numbers of corresponding bond types are similar to each other, there being only a minor difference during solidification processes.

Although HA bond-type indices can be used successfully for the description of the bonding relationship between an atom and its nearest neighbours, they still cannot describe the different basic clusters formed by an atom with its nearest neighbours. This inability is particularly evident in the analysis of nanoclusters formed by different basic clusters, as shown below.

3.3. Cluster-type index analyses

In order to differentiate the basic cluster and the polyhedron, we define the basic cluster as the smallest cluster composed of a core atom and its surrounding neighbour atoms. A larger cluster can be formed by continuous expansion, with a basic cluster as the core, according to a certain rule, or by combining several basic clusters together. A polyhedron is generally a hollow structure with no central atom as the core. This is the essential distinction of a polyhedron from a basic cluster, such as the Bernal polyhedron. However, if a basic cluster is shaped as a certain polyhedron, for simplicity, we also call it a polyhedron cluster, such as icosahedral cluster, Bernal polyhedron cluster, and so on.

It is clear that the bond types formed by each atom with its neighbour atoms in the system are different; the cluster configurations formed by these bond types are also different. Even if some cluster configurations are formed by the same number of bond types, their structures may still be completely different from each other, owing to a slight difference in bond length or bond angle. On this point, it is hard to use the bond-type index method at present to describe clearly the cluster configurations of different types. In order to deal with this difficult matter, a cluster-type index method (CTIM) has been proposed [17–21] based on the HA indices [27] and the work of Qi and Wang [29]. According to the definition of a basic cluster, four integers are also adopted to describe the basic clusters. The meaning of the four integers used in CTIM are as follows: the first integer represents the number of surrounding atoms which form a basic cluster with the central atom, i.e. the coordination number Z of the central atom; the second, third and

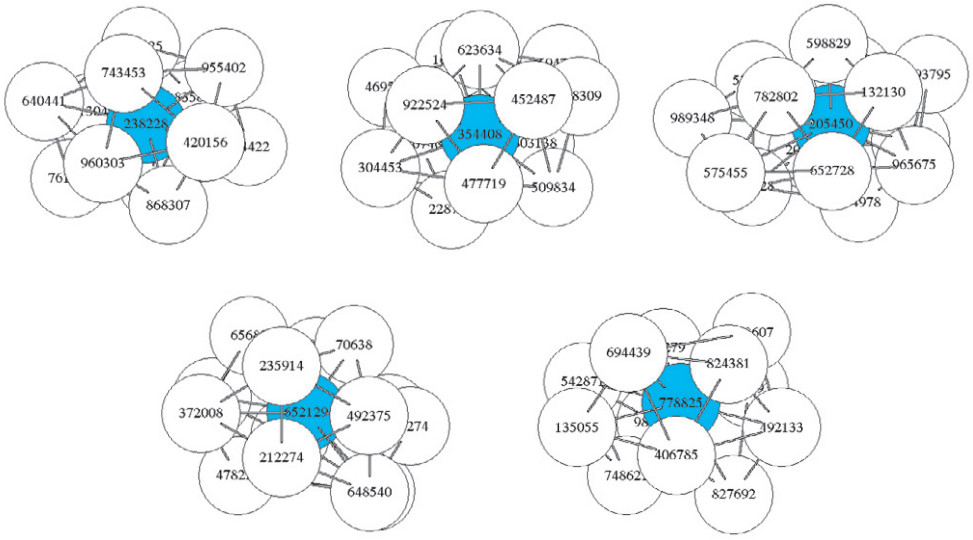

Figure 2. Schematics of five main basic clusters at 350 K: (a) icosahedral cluster (12 0 12 0) with central atom of 238228; (b) basic cluster (13 1 10 2) with central atom of 354408; (c) basic cluster (14 2 8 4) with central atom of 205450; (d) basic cluster (14 1 10 3) with central atom of 652129; (e) basic cluster (12 2 8 2) with central atom of 778825.

fourth integers respectively represent the number of 1441, 1551 and 1661 bond types, by which the surrounding atoms are connected with the central atom of the basic cluster. For example, (12 0 12 0) stands for an icosahedral cluster that is composed of 13 atoms: the central atom is connected to the surrounding atoms through twelve 1551 bond types (i.e. the coordination number of the central atom $Z = 12$); (13 1 10 2) stands for the defective polyhedron cluster composed of 14 atoms: the core atom is connected to the surrounding atoms with one 1441, ten 1551 and two 1661 bond types (the coordination number $Z = 13$). Briefly, we only selected five main basic clusters from this simulation system as shown in figure 2.

Based on this definition of the CTIM, the statistical numbers of various cluster types at each given temperature have been obtained; during the whole solidification process, there are 53 different basic cluster types in the system, only 34 of them appearing more than five times at some temperatures are listed in table 2. From table 2, however, it can be clearly seen that only 18 cluster types appearing more than 100 times play a critical role in the solidification process. For convenience of discussion, we only show the variations of ten significant basic clusters with temperature in figure 3.

From figure 3(a), it is clear that among the most significant five basic clusters, the most frequently occurring one is the icosahedral basic cluster expressed by (12 0 12 0), which increases rapidly as the temperature comes down. The number of basic cluster (12 0 12 0) reaches more than 30 000 at 350 K, and this cluster type plays the most important role in the microstructure transitions during rapid solidification process. The second most frequently occurring is the basic cluster expressed by (13 1 10 2) and its number is over 9400 at 350 K. The number of the fifth cluster type, expressed by (12 2 8 2), is over 1956 at 350 K and still plays a certain role.

Figure 3(b) shows that the numbers of basic clusters (14 0 12 2), (15 1 10 4), (13 2 8 3) and (15 2 8 5) all changed at about the same rate, except the basic cluster (13 3 6 4), and their numbers are in the range of 1023–1360 at 350 K. Therefore, these clusters play only a secondary role.

Table 2. Variation of the number of clusters with temperature (K).

Types of cluster	Temperature (K) and the number of various cluster types											
	943	883	833	780	730	675	625	550	500	450	400	350
(12 0 12 0)	2106	2819	3671	4867	6389	8698	10 833	14 857	18 328	22 216	26 207	30 153
(14 0 12 2)	183	210	253	368	447	564	751	881	1 007	1 189	1 203	1 360
(15 0 12 3)	78	68	103	126	165	208	262	358	410	391	478	472
(16 0 12 4)	8	19	17	27	31	40	34	46	55	63	74	83
(13 1 10 2)	1544	1919	2341	3078	3750	4870	5 357	6 522	7 244	8 125	8 974	9 417
(14 1 10 3)	427	536	684	894	1113	1366	1 585	1 881	2 136	2 382	2 638	2 892
(15 1 10 4)	172	213	285	366	452	568	647	845	899	1 026	1 092	1 117
(16 1 10 5)	29	37	42	67	76	95	104	111	127	136	163	175
(17 1 10 6)	2	6	2	4	4	3	6	9	5	7	4	5
(10 2 8 0)	13	7	16	13	15	11	12	3	5	2	2	0
(11 2 8 1)	231	243	260	269	273	274	250	215	188	173	148	110
(12 2 8 2)	969	1066	1208	1440	1624	1865	1 974	2 117	2 037	2 067	2 051	1 956
(13 2 8 3)	396	452	548	585	740	882	933	960	1 051	1 029	999	1 035
(14 2 8 4)	735	865	1014	1291	1632	1992	2 194	2 635	2 758	2 985	3 286	3 363
(15 2 8 5)	188	224	288	346	415	573	619	750	810	791	939	1 023
(16 2 8 6)	23	26	52	59	56	75	86	94	77	102	110	122
(17 2 8 7)	0	3	2	6	5	5	7	8	4	0	2	3
(10 3 6 1)	3	6	5	2	1	5	4	3	1	1	1	0
(11 3 6 2)	41	36	38	33	29	23	19	19	20	13	5	8
(12 3 6 3)	288	260	301	359	375	345	322	253	276	199	174	140
(13 3 6 4)	914	1016	1191	1412	1651	1810	1 951	1 936	1 884	1 857	1 782	1 689
(14 3 6 5)	318	400	527	570	669	739	800	845	884	834	853	868
(15 3 6 6)	103	106	149	182	227	224	295	267	358	330	364	371
(16 3 6 7)	11	9	13	12	14	28	25	28	29	30	25	27
(11 4 4 3)	19	16	21	13	21	16	15	11	6	5	2	2

Table 2. (Continued.)

Types of clusters	Temperature (K) and the number of various cluster types											
	943	883	833	780	730	675	625	550	500	450	400	350
(12 4 4 4)	102	106	83	80	95	88	89	63	47	55	33	33
(13 4 4 5)	131	112	124	151	133	192	149	131	102	107	85	65
(14 4 4 6)	175	225	226	261	266	332	354	336	311	258	268	269
(15 4 4 7)	42	56	59	58	62	76	105	101	88	84	113	83
(16 4 4 8)	5	5	3	6	3	7	10	10	9	6	5	13
(12 5 2 5)	7	9	17	10	11	3	8	5	4	2	1	2
(13 5 2 6)	27	30	33	30	40	30	30	39	15	18	23	17
(15 5 2 8)	1	4	1	7	5	6	5	7	12	2	5	4
(14 6 0 8)	4	2	6	8	3	8	9	9	5	4	1	3
Total number of all clusters	9300	11 117	13 589	17 006	20 796	26 029	29 854	36 365	41 203	46 498	52 122	56 885
Icosahedra expressed by (12 0 12 0) related to the total number of all clusters (%)	22.65	25.36	27.01	28.62	30.72	33.42	36.29	40.85	44.48	47.78	50.28	53.01

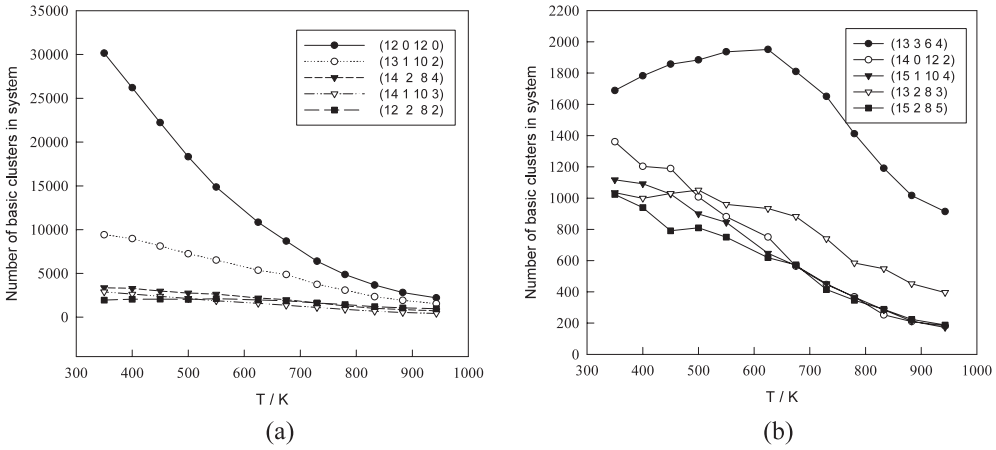

Figure 3. Variation of the numbers of the ten main basic clusters with temperature.

However, as we go further to observe figures 3(a), (b) and table 2 carefully, it can be seen that the basic clusters (12 0 12 0) and (13 3 6 4) have almost a same turning point T_t in the range of 550–625 K; in particular for cluster (13 3 6 4), T_t is a peak value point, which means that the cluster (13 3 6 4) plays an opposite role to the cluster (12 0 12 0) in the solidification process. Maybe just these cluster types play a particular role; this turning point T_t is in agreement with the glass transition temperature T_g obtained by Liu *et al* [30, 31]. On the other hand, this confirms that the glass transition temperature T_g can also be found by the turning point T_t in the relations of the numbers of main basic clusters with temperature. Therefore, it is possible to find a new method to determine the glass transition temperature T_g.

It is worth noting that, from table 2, it can be clearly seen that, even at 943 K, there are still a certain number of various basic clusters in the liquid state. That is to say, the liquid state discussed here is not an ideal liquid, as usually imagined, in which no clusters exist and each atom is free to diffuse. Furthermore, from our previous works for a small system consisting of 500 Al atoms, as shown in figure 3 of [32], it can be seen that even when the temperature is increased up to 1800 K ($\approx 2T_m$), the number of 1551 bond types (which play a leading role in the microstructure transition of liquid metal Al) is still 7.3% of the total number of bond types (and 16.5% at 943 K); thus some basic clusters formed mainly by the 1551 bond type would still be in the liquid system. If we want to get an ideal liquid state, the temperature should be increased higher and higher. In general, from the viewpoint of microscopic structure, it is hard to completely reach the ideal case.

3.4. Formation and description of nanoclusters

Before discussing the description of nanoclusters, we show in figure 4 a schematic diagram of the cross section of the 10^6 atom system at 350 K. Figure 4(a) shows a quarter of the real (111) cross section (not a projection) of the simulation system and figure 4(b) shows 1/16 of its enlarged section. In the cross section, the full spots are just through the centre of atoms and the small spots partially cut the atoms. From figure 4, it can be clearly seen that the system has become an amorphous state and that dense and loose regions have formed. In the dense regions, there are some cluster structures of different sizes and shapes, in which atoms are arranged according to a certain rule and possess short-range-order characteristics. In particular, it is clear that some regular or distorted five-fold patterns appear, as shown in figure 4(b); these

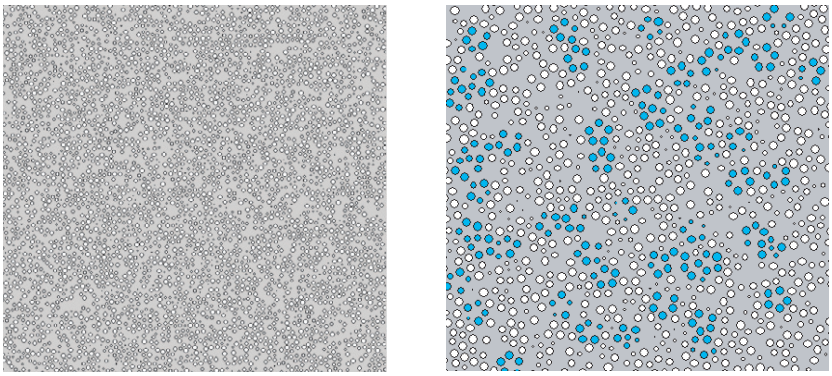

(a) (b)

Figure 4. A two-dimensional schematic diagram of the whole system consisting of 1000 000 atoms at 350 K: (a) 1/4 of the (111) cross section; (b) 1/16 of the (111) cross section.

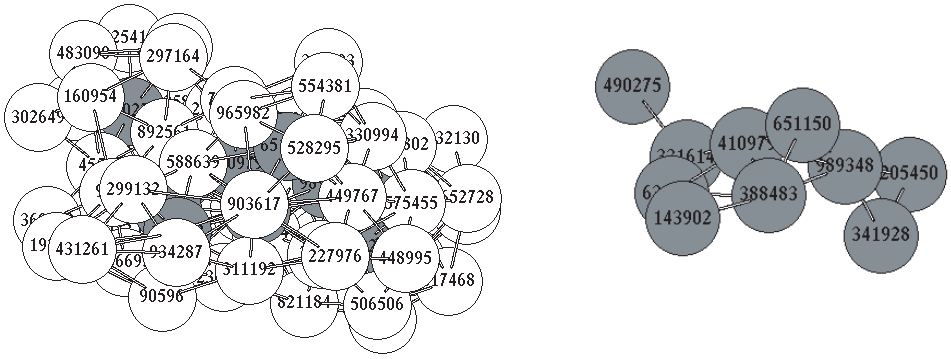

(a) (b)

Figure 5. Schematic diagram of a larger cluster consisting of 68 atoms within ten basic clusters with connecting bonds at 350 K (the grey spheres are the centre atoms of basic clusters). The cluster is composed of one icosahedron (12 0 12 0), and basic clusters of one (16 0 12 4), five (13 1 10 2), one (14 1 10 3), one (14 2 8 4) and one (14 3 6 5). (a) displays all the atoms; (b) displays only the central atoms.

are just the cross sections of some icosahedra and their combining configurations as shown in green (or grey in the printed version).

The loose regions are also of different sizes and shapes without apparent regulation and the atoms are randomly distributed there. The dense regions and the loose regions are also distributed randomly in the system; the inhomogeneous solid seems to be rather sponge-like with cavities (also commonly called 'free volume') in different sizes and shapes. It is clear that it is hard to describe the microstructure of this system by the well-known model of 'random hard-sphere packing', since that model is too simple for describing amorphous metals. Figure 4, however, shows a typical amorphous picture; thus it is necessary to establish a new model to describe the complex structures of amorphous metals in the near future.

In this simulation, some larger clusters have been found. They are composed of various kinds of basic clusters and their sizes and numbers increase with temperature decreasing. Their configurations are very complex. For example, a larger cluster consisting of 68 atoms is composed of ten basic clusters with central atoms (represented by grey circles) as shown in figures 5(a) and (b), displaying the whole atoms and the central atoms, respectively. From

figures 5(a) and (b), it can be clearly seen that the larger cluster is formed by combining different medium-sized clusters, and each medium-sized cluster is also composed of some basic clusters that can be described by a set of indices in the CTIM, as shown in the caption. Interestingly, the larger clusters formed during rapid solidification processes of liquid metal Al do not consist of multi-shell configurations accumulated by atoms as obtained by gaseous deposition or ionic spray methods. However, the cluster configurations of Al formed by gaseous deposition have been verified by mass spectrometry to be crystals or similar structures formed in octahedral shell structures [33]. Therefore, it can be concluded that different methods of preparing metallic materials would produce different cluster configurations. Figure 5 shows that the atoms contained in the larger clusters are labelled randomly; that is to say, the atoms in the system have been distributed homogeneously.

3.5. Size distribution and magic number characteristics of clusters

In order to investigate the size distribution of various clusters in the system, the relationship between the numbers of various clusters and their sizes (the numbers of atoms contained in each cluster) should be displayed clearly according to some statistical method. For convenience of discussion, we propose a new statistical method as follows.

Since a larger cluster can be described clearly by different basic clusters in the CTIM, all the clusters (from basic cluster to larger cluster) in the system can be classified according to the numbers of basic clusters contained in the larger cluster under consideration. Then, the clusters containing the same numbers of basic clusters can be further classified as a group. However, the clusters within a same group may not have the same numbers of atoms because the different basic clusters they contain would have different numbers of atoms. Thus there is a certain range of the numbers of atoms for a group of clusters; this can be clearly seen below. For simplicity, we only analyse ten groups in the system in turn by the numbers of basic clusters contained in each group for two cases of liquid state at 943 K and solid state at 350 K, as shown in table 3. From table 3, it can be clearly seen that there is a peak value (maximum) of the numbers of clusters for each group, and this is shown with a short underline in the table. As we compare this peak value with the abundance usually used in the research of cluster configurations, it is found that the two concepts are completely consistent with each other. As we display the relations of the numbers of clusters formed in the system with the size (the number of atoms contained in them) of these clusters, it is further found that the positions of the peak value points of the numbers of clusters also correspond to the magic number points. It is also clearly seen that the numbers of clusters at 943 K are much less than those for the same group level at 350 K for the former five group levels and there are few or almost none for the latter five group levels, and the front five peak value positions of clusters at 943 K are not all consistent with those at 350 K; for convenience of discussion for magic numbers, we only show the simulation results at 350 K in figure 6.

It is clear from figure 6 that the quantity of the various clusters is sensitive to the size of the cluster, and that magic numbers do exist. In the solid state at 350 K, the total magic number sequence of all groups is in turn as 13, 19, 25, 27, 31, 33, 38, 40, 42, 45, 48, 51, 59, 65, 67 . . .. However, when the number of atoms contained in a cluster is more than 70, the position of its magic number would be ambiguous.

In order to further reveal the magic number characteristics of the above-mentioned groups, we show the variation of the numbers of clusters in the system with the numbers of atoms contained in the clusters for ten groups in figure 7(a), (b) and (c), respectively.

It is observed in figure 7 that although the ranges of neighbouring groups have overlapped each other, one or two partial magic numbers still can be obviously distinguished for each

Table 3. Relationships of the numbers of clusters consisting of 1–10 basic clusters with the cluster size (number of atoms included).

Cluster consisting of 1 basic cluster			Cluster consisting of 2 basic clusters			Cluster consisting of 3 basic clusters			Cluster consisting of 4 basic clusters			Cluster consisting of 5 basic clusters		
Cluster size	Cluster number		Cluster size	Cluster number		Cluster size	Cluster number		Cluster size	Cluster number		Cluster size	Cluster number	
Number of atoms	943 K	350 K	Number of atoms	943 K	350 K	Number of atoms	943 K	350 K	Number of atoms	943 K	350 K	Number of atoms	943 K	350 K
11	13	0	17	1	0	23	9	210	26	0	7	30	0	2
12	245	55	18	6	4	24	19	204	27	0	27	31	0	6
13	2254	10 606	19	167	2761	25	28	647	28	2	47	32	0	9
14	1912	3 159	20	269	1432	26	53	551	29	4	130	33	1	23
15	998	1 611	21	311	1370	27	62	588	30	10	128	34	3	46
16	300	433	22	202	730	28	43	451	31	8	212	35	0	69
17	39	37	23	86	273	29	32	202	32	9	210	36	4	69
18	0	1	24	46	56	30	21	106	33	10	225	37	1	105
			25	13	15	31	3	38	34	7	194	38	7	118
			26	2	1	32	4	15	35	15	126	39	6	106
						33	1	3	36	3	83	40	0	110
									37	4	27	41	2	69
									38	1	17	42	1	46
									39	1	7	43	1	27
									40	0	1	44	1	15
									41	0	1	45	0	7
									42	0	2	46	0	5
												47	0	2

Table 3. (Continued.)

Cluster consisting of 6 basic clusters			Cluster consisting of 7 basic clusters			Cluster consisting of 8 basic clusters			Cluster consisting of 9 basic clusters			Cluster consisting of 10 basic clusters		
Cluster size	Cluster number		Cluster size	Cluster number		Cluster size	Cluster number		Cluster size	Cluster number		Cluster size	Cluster number	
Number of atoms contained	943 K	350 K	Number of atoms contained	943 K	350 K	Number of atoms contained	943 K	350 K	Number of atoms contained	943 K	350 K	Number of atoms contained	943 K	350 K
35	0	2	37	0	1	44	0	1	46	0	1	56	0	2
36	0	3	38	0	0	45	0	0	47	0	0	57	0	1
37	0	7	39	0	0	46	0	1	48	0	0	58	0	1
38	1	7	40	0	0	47	0	2	49	0	2	59	0	1
39	2	16	41	0	4	48	0	4	50	0	0	60	0	2
40	0	34	42	1	3	49	0	3	51	0	0	61	0	1
41	1	36	43	1	8	50	1	8	52	0	3	62	0	7
42	2	54	44	0	13	51	0	12	53	0	0	63	0	5
43	0	51	45	0	12	52	0	11	54	0	4	64	0	4
44	2	33	46	0	19	53	0	13	55	0	6	65	0	3
45	0	51	47	0	23	54	0	16	56	0	3	66	0	4
46	0	45	48	2	33	55	0	17	57	0	7	67	0	9
47	0	21	49	1	17	56	0	16	58	0	5	68	0	6
48	0	27	50	0	27	57	0	10	59	0	5	69	0	6
49	0	12	51	0	29	58	0	13	60	0	7	70	0	2
50	0	9	52	0	20	59	0	22	61	0	9	71	0	0
51	0	8	53	0	18	60	0	11	62	0	3	72	0	1
52	0	1	54	0	12	61	0	6	63	0	7	73	0	1
53	0	1	55	0	6	62	0	3	64	0	2	74	0	2

Table 3. (Continued.)

Cluster consisting of 6 basic clusters			Cluster consisting of 7 basic clusters			Cluster consisting of 8 basic clusters			Cluster consisting of 9 basic clusters			Cluster consisting of 10 basic clusters		
Cluster size	Cluster number		Cluster size	Cluster number		Cluster size	Cluster number		Cluster size	Cluster number		Cluster size	Cluster number	
Number of atoms contained	943 K	350 K	Number of atoms contained	943 K	350 K	Number of atoms contained	943 K	350 K	Number of atoms contained	943 K	350 K	Number of atoms contained	943 K	350 K
			56	1	4	63	0	0	65	0	14	75	0	1
			57	0	4	64	0	1	66	0	4	76	0	0
			58	0	3	65	0	1	67	0	1	77	0	0
			59	0	1	66	0	1	68	0	6	78	0	1
									69	0	1			
									70	0	2			
									71	0	0			
									72	0	0			
									73	0	0			
									74	0	0			
									75	0	1			

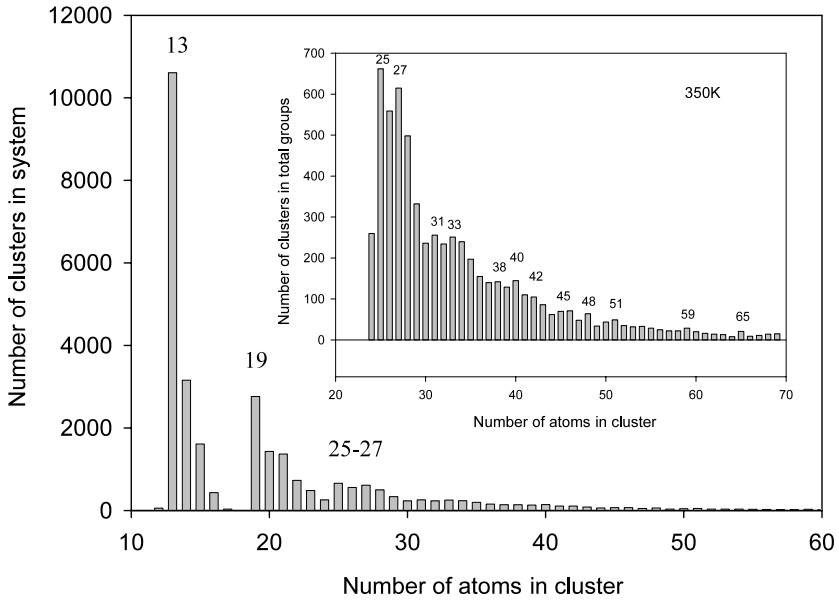

Figure 6. Variation of the numbers of clusters in the system with sizes of clusters (i.e. the number of atoms contained in the cluster) at 350 K.

group, and all the partial magic numbers for the ten groups rather correspond to the total magic number sequence for the whole system as shown in figure 6. Going further, the total magic number sequence can be classified again according to the order of the ten groups of clusters in the following sequence: 13 (first magic number), 19 (second), 25–27 (third), 31–33 (fourth), 38–40 (fifth), 42–45 (sixth), 48–51 (seventh), 55–59 (eighth), 61–65 (ninth) and 67 (tenth). The ninth and tenth magic numbers are not so obvious in figure 6 because the numbers of clusters containing nine and ten basic clusters are insufficient; however, they stand out in figure 7(c). For simplicity, the magic number sequence corresponding to the order of the ten groups of clusters can be listed again as 13, 19, 25 (27), 31 (33), 38 (40), 42 (45), 48 (51), 55 (59), 61 (65) and 67, where the numbers in brackets are the secondary magic numbers of the corresponding groups of clusters. We think the above-mentioned analysis is very important in searching for the origin of the magic numbers of clusters formed in the system.

We compare the total magic number sequence mentioned above to the experimental results of the photo-ionization mass spectra of clusters, formed through supersonic deposition from supersaturated gaseous phase Al, obtained by Schriver *et al* as shown in figure 3 of [4]; it can be clearly seen that the magic numbers reported (14, 17, 23, 29, 37, 43, 47, 55, 67 . . .), and those not reported (19, 21, 25, 33, and 39) (they can be clearly seen in the same figure 3; perhaps the authors thought that those numbers were not consistent with the magic number rule at that time), are almost all consistent with our magic number sequence (in the error range of ± 1). Thus, it can be said that the magic number sequence from our simulation is supported by the experimental results, but their clusters are produced by both different formation processes even though they are of the same element, Al.

In particular, as we further compare the magic number sequence from our simulation to the experimental results of inert gas clusters, it can also be clearly seen that the magic number sequence obtained from the mass spectra of Ar clusters formed in a supersaturated ionic phase given by Harris *et al* is 13, 19, 23, 26, 29, 32, 34, 43, 46, 49, 55, 61, 64, 66 . . . (see

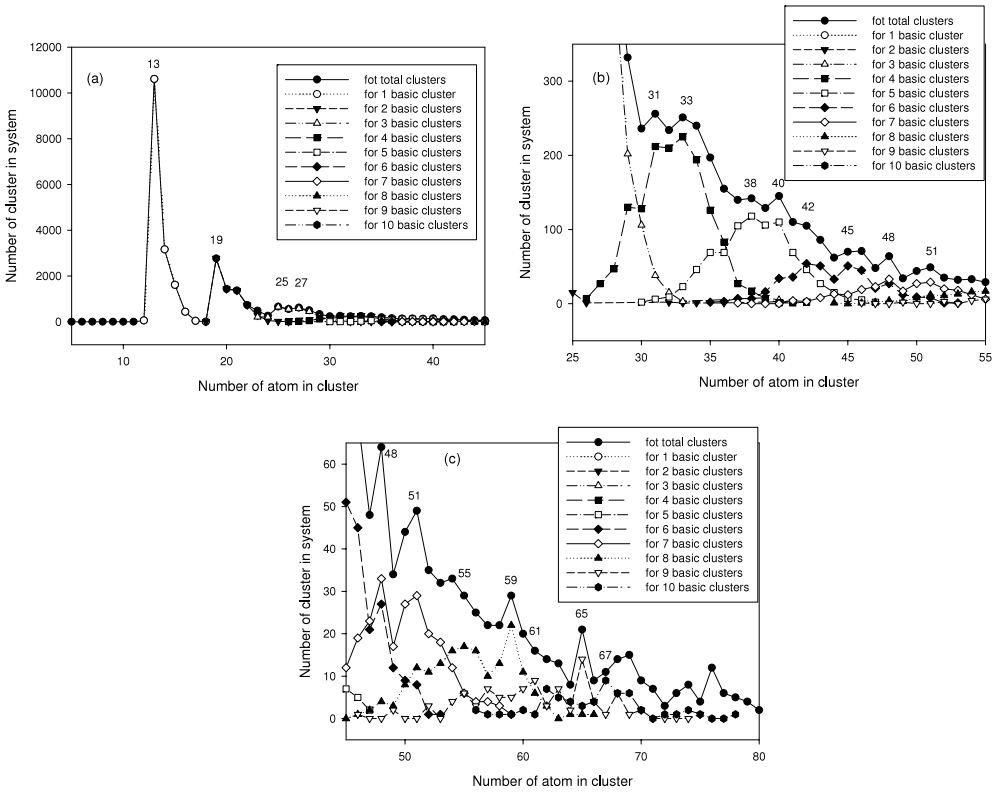

Figure 7. Relationship of the numbers of basic clusters contained in a group level of clusters with the size of the cluster (number of atoms contained in the cluster) at 350 K. (a) for 1st–3rd group; (b) for 4th–6th group; (c) for 7th–10th group levels of clusters.

figure 1 in [2]), and the sequence obtained from the mass spectra of Xe clusters formed in a supersaturated vapour phase given by Echt *et al* [3] is 13, 19, 23, 25, 29, 55, 71 . . . (see figure 1 in [3]); these results are also in good agreement with our sequence in the same error range. That is to say that this simulation result from metal Al is similar to those from inert gases Ar and Xe, and this similarity should reflect to a certain degree some essential relations between different elements, especially in different states.

It is highly interesting that this magic number sequence is also in good agreement with the results obtained by using MD simulation and other model potentials from Solov'yov's and Doye's works, such as 13, 19, 23, 26, 29, 32, 34, 43, 46, 49, 55, 61, 64, 71, . . . (see figures 1 and 2 in [12]), and 13, 19, 23, 26, 29, 34, 45, 51, 55, . . . (see figures 1 and 2 in [13]), respectively. From these, it can be explained that as long as the methods used to solve the similar problem are reasonable, the results should also be similar.

Going further, it can be seen that not only have the experimental results reported by Schriver and Harris *et al* [2, 4] provided a vital experimental certification of our simulation results, but also our simulation results could provide a reasonable model explanation of those experimental results. As regards the magic numbers obtained from experimental researches, some of them can be explained as usual from the viewpoint of the geometric shell structure of cluster configurations being closed regularly (for neutral clusters and charged clusters) [1–5], but the others cannot be explained from the same viewpoint because they correspond to the geometric non-shell structure of cluster configurations. However, from our simulation, it can be

clearly seen that during the forming process of larger clusters, only a few clusters accumulate and extend continuously with a basic cluster as the core according to a certain rule; most of them are formed by combining different numbers and different types of basic clusters. So, this is the normal case and it can be used to find more clusters with geometric non-shell structure in their magic number sequence as noted above.

So far, the critical question is why the magic number sequence of clusters formed by solidification of liquid metal Al from our simulation is so similar to those magic number sequences of clusters formed by ionic spray and gaseous deposition of metal Al, and inert gases Ar and Xe from experimental studies. We think the main reason is that the solidification process of liquid metal is essentially similar to the formation process of clusters in the above-mentioned experimental studies. We consider that in the solidification process of liquid metals, various cluster configurations could be formed by the rapid agglomerating of a large number of atoms as the system spreads over a large space for a short time, while in the formation process of clusters in the experiments, various cluster configurations could be formed by slow gathering of a few atoms as the system spreads over a small space for a long time, and both their final results could be similar to each other on the whole (even though they are not completely similar). On the other hand, at present, the essential differences between different elements, and especially different states, can still not be distinguished in detail; it is necessary to analyse and compare in detail various similar and dissimilar magic numbers of these sequences in the future.

Therefore, it may be feasible to adopt magic numbers, especially the partial magic numbers of the group levels, obtained during the rapid solidification process of liquid metals to understand the magic number characteristics obtained with experimental methods.

4. Conclusions

In this paper, in order to investigate the formation and magic number characteristics of various clusters formed during solidification processes, a molecular dynamic simulation study has been performed for a large-sized system consisting of 10^6 liquid metal Al atoms. The cluster-type index method (CTIM) is adopted to describe various types of cluster by basic clusters. It is demonstrated that the icosahedral cluster (12 0 12 0) is the most important basic cluster, and it plays a critical role in the microstructure transition. A new statistical method has been proposed to classify the clusters formed in the system by the numbers of basic clusters contained in each cluster, and the clusters consisting of the same numbers of basic clusters but not the same numbers of atoms can be classified as a group level of clusters. In each group level, the peak value position of the numbers of cluster corresponds to the partial magic number of that group level. The total magic number sequence of the system is composed of all the partial magic numbers of various group levels and can be listed as 13, 19, 25 (27), 31 (33), 38 (40), 42 (45), 48 (51), 55 (59), 61 (65) and 67, where the numbers in brackets are the secondary magic numbers (peak value positions) of the corresponding group levels of clusters. This magic number sequence is in good agreement with the experimental results obtained by Schriver and Harris *et al*. This method of determining the magic numbers, especially the partial magic numbers, can be used to provide a reasonable explanation of those experimental results.

Acknowledgments

This work was supported by the National Natural Science foundation of China (Grant No 50271026, 50571037), and KJD and ABY are grateful to the Australian Research Council (ARC) for financial support through the ARC Centre for Functional Nanomaterials.

References

[1] Knight W D *et al* 1984 *Phys. Rev. Lett.* **52** 2141
[2] Harris I A, Kidwell R S and Northby J A 1984 *Phys. Rev. Lett.* **53** 2390
[3] Echt O, Sattler K and Recknagle E 1981 *Phys. Rev. Lett.* **47** 1121
[4] Schriver K E *et al* 1990 *Phys. Rev. Lett.* **64** 539
[5] Robles R, Longo R C and Vega A 2002 *Phys. Rev.* B **66** 064410
[6] Magudapathy P *et al* 2001 *Physica* B **299** 142
[7] Spiridis N, Haber J and Korecki J 2001 *Vacuum* **63** 99
[8] Liu X H *et al* 1998 *Chem. Phys. Lett.* **288** 804
[9] Yamamoto H and Asaoka H 2001 *Appl. Surf. Sci.* **169/170** 305
[10] Bruhl R *et al* 2004 *Phys. Rev. Lett.* **92** 185301
[11] Liu C S *et al* 2001 *J. Phys.: Condens. Matter* **13** 1873
[12] Solov'yov I A, Solov'yov A V and Greiner W 2003 *Phys. Rev. Lett.* **90** 053401
[13] Doye J P K and Meyer L 2005 *Phys. Rev. Lett.* **95** 063401
[14] Li H and Pederiva F 2003 *Phys. Rev.* B **68** 054210
[15] Ikeshoji T *et al* 1996 *Phys. Rev. Lett.* **76** 1792
[16] Wang L, Bian X F and Zhang J X 2002 *Modelling Simul. Mater. Sci. Eng.* **10** 331
[17] Liu R S, Li J Y and Zhou Q Y 1995 *Chin. Sci. Bull.* **40** 1429
[18] Liu R S *et al* 2002 *Mater. Sci. Eng.* B **94** 141
[19] Dong K J *et al* 2003 *J. Phys.: Condens. Matter* **15** 743
[20] Liu R S *et al* 2005 *J. Non-Cryst. Solids* **351** 612
[21] Liu R S *et al* 2005 *Sci. China* G **48** 101
[22] Qi D W and Wang S 1991 *J. Non-Cryst. Solids* **135** 73
[23] Wang S and Lai S K 1980 *J. Phys. F: Met. Phys.* **10** 2717
[24] Li D H, Li X R and Wang S 1986 *J. Phys. F: Met. Phys.* **16** 309
[25] Hoover W G, Ladd A J C and Moran B 1982 *Phys. Rev. Lett.* **48** 1818
[26] Evans D J 1983 *J. Chem. Phys.* **78** 3297
[27] Honeycutt J D and Andersen H C 1987 *J. Phys. Chem.* **91** 4950
[28] Waseda Y 1980 *The Structure of Non-Crystalline Materials* (New York: McGraw-Hill) p 270
[29] Qi D W and Wang S 1991 *Phys. Rev.* B **44** 884
[30] Wendt H R and Abraham F F 1978 *Phys. Rev. Lett.* **41** 1244
[31] Liu R S, Qi D W and Wang S 1992 *Phys. Rev.* B **45** 451
[32] Liu R S *et al* 1999 *Mater. Sci. Eng.* B **57** 214
[33] Martin T P, Naher U and Schaber H 1992 *Chem. Phys. Lett.* **199** 470